

Article

Isolation and Identification of Pentalenolactone Analogs from *Streptomyces* sp. NRRL S-4

Huanhuan Li ^{1,2,†}, Hongji Li ^{1,†}, Shuo Chen ^{1,2}, Wenhui Wu ^{2,*}  and Peng Sun ^{1,*} 

¹ Department of Phytochemistry, School of Pharmacy, Second Military Medical University, 325 Guo-He Road, Shanghai 200433, China; m13083766175@163.com (H.L.); lihongji0327@smmu.edu.cn (H.L.); m190310884@st.shou.edu.cn (S.C.)

² Department of Marine Bio-Pharmacology, College of Food Science and Technology, Shanghai Ocean University, 999 Huchenghuan Road, Shanghai 201306, China

* Correspondence: whwu@shou.edu.cn (W.W.); sunpeng78@126.com (P.S.); Tel.: +86-21-81871259 (P.S.)

† These authors contributed equally to this work.

Abstract: Terpene synthases are widely distributed in Actinobacteria. Genome sequencing of *Streptomyces* sp. NRRL S-4 uncovered a biosynthetic gene cluster (BGC) that putatively synthesizes pentalenolactone type terpenes. Guided by genomic information, the S-4 strain was chemically investigated, resulting in the isolation of two new sesquiterpenoids, 1-deoxy-8 α -hydroxypentalenic acid (**1**) and 1-deoxy-9 β -hydroxy-11-oxopentalenic acid (**2**), as shunt metabolites of the pentalenolactone (**3**) biosynthesis pathway. Their structures and absolute configurations were elucidated by analyses of HRESIMS and NMR spectroscopic data as well as time-dependent density functional theory/electronic circular dichroism (TDDFT/ECD) calculations. Compounds **1** and **2** exhibited moderate antimicrobial activities against Gram-positive and Gram-negative bacteria. These results confirmed that the pentalenolactone pathway was functional in this organism and will facilitate efforts for exploring Actinobacteria using further genome mining strategies.

Keywords: *Streptomyces*; pentalenolactone; terpenoid; genome mining; secondary metabolites



Citation: Li, H.; Li, H.; Chen, S.; Wu, W.; Sun, P. Isolation and Identification of Pentalenolactone Analogs from *Streptomyces* sp. NRRL S-4. *Molecules* **2021**, *26*, 7377. <https://doi.org/10.3390/molecules26237377>

Academic Editors: Brian T. Murphy and Hendrik Luesch

Received: 29 October 2021

Accepted: 1 December 2021

Published: 5 December 2021

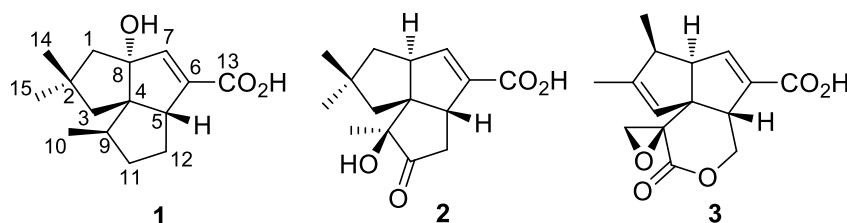
Publisher's Note: MDPI stays neutral with regard to jurisdictional claims in published maps and institutional affiliations.



Copyright: © 2021 by the authors. Licensee MDPI, Basel, Switzerland. This article is an open access article distributed under the terms and conditions of the Creative Commons Attribution (CC BY) license (<https://creativecommons.org/licenses/by/4.0/>).

1. Introduction

Actinobacteria have been proven to be one of the most reliable sources of natural products with industrial and medicinal importance. Whole-genome sequencing and bioinformatics analyses reveal an enormous number of secondary metabolite biosynthetic gene clusters (BGCs) in Actinobacteria [1]. Given that genes encoding terpene synthases have been found to be widely distributed [2], it is believed that the amount of terpene metabolites currently reported in Actinobacteria is an underestimation. Genome mining approaches have greatly enhanced the discovery of secondary metabolites from Actinobacteria [3]. In the course of our ongoing search for bioactive metabolites from marine invertebrates and microorganisms [4–6], the strain *Streptomyces* sp. NRRL S-4 (S-4) was selected for the exploration of secondary metabolite profiles. Previous studies of this strain resulted in the discovery of thiostreptamides and venturicidins [6,7]. Whole-genome sequencing revealed that S-4 contained 25 BGCs including six BGCs that putatively synthesized the terpenoids [6]. Aiming at terpenoid metabolites, we chemically investigated the organic extracts of S-4 fermentation and discovered two new sesquiterpenoids, 1-deoxy-8 α -hydroxypentalenic acid (**1**) and 1-deoxy-9 β -hydroxy-11-oxopentalenic acid (**2**). Herein, we reported the isolation, elucidation, and biological activities of these compounds.



2. Results

2.1. Pentalenolactone BGC in S-4

The whole genome of S-4 was 7.4-Mb in size. With online antiSMASH analysis, a total of 25 putative secondary metabolite BGCs were predicted including six terpene BGCs (Table S1) [8]. One terpene BGC, here designated as the *pll* cluster, possibly synthesized the pentalenolactone (3) metabolites. The 12.9-kb *pll* BGC consisted of 10 open reading frames (ORFs) showing an average >90% sequence similarity to those of the *pnt* BGC from validated pentalenolactone producer *S. arenae* [9]. (Table 1) The ORFs of the *pll* BGC were identical in organization to those of the *pnt* BGC. In silico genome analysis implied the possibility of finding pentalenolactone or its derivatives in the S-4 culture broth.

Table 1. Deduced functions of ORFs in *pll* BGC of S-4.

Protein	Size (aa)	Protein Homologue and Origin	Identity/Similarity, %/%	Proposed Function
PIIN	334	GapR, <i>S. arenae</i> TU469	93/100	glyceraldehyde-3-phosphate dehydrogenase
PIIM	398	PntM, <i>S. arenae</i> TU469	87/100	cytochrome P450 monooxygenase
PIIH	283	PntH, <i>S. arenae</i> TU469	89/100	1-deoxypentalenic acid-11-beta-hydroxylase
PIIG	484	PntG, <i>S. arenae</i> TU469	84/99	transmembrane efflux protein
PIIF	275	PntF, <i>S. arenae</i> TU469	91/91	short-chain dehydrogenase/reductase
PIIE	584	PntE, <i>S. arenae</i> TU469	91/100	Baeyer-Villiger monooxygenase
PIID	299	PntD, <i>S. arenae</i> TU469	89/100	non-heme iron/alpha-ketoglutarate-dependent dioxygenase
PIIB	337	PntB, <i>S. arenae</i> TU469	93/99	polyprenyl diphosphate synthase
PIIA	337	PntA, <i>S. arenae</i> TU469	100/100	pentalenene synthase
PIII	457	PntI, <i>S. arenae</i> TU469	92/97	cytochrome P450 monooxygenase

2.2. Isolation and Structural Identification

Compound 1 was isolated as an amorphous powder. Its molecular formula was determined to be $C_{15}H_{22}O_3$ on the basis of high-resolution electrospray ionization mass spectrometry (HRESIMS) at m/z : 249.1489 $[M - H]^-$ (calcd for $C_{15}H_{21}O_3$, 249.1485), requiring five double-bond equivalents (DBE). The IR spectrum displayed absorptions for hydroxy (3377 cm^{-1}) and α , β -unsaturated carboxylic acid (1684 cm^{-1}) functionalities. The ^{13}C -NMR and distortionless enhancement by polarization transfer (DEPT) spectra displayed 15 signals which corresponded to 3 sp^2 (1 C=O, 1 C=CH) and 12 sp^3 (3 CH_3 , 4 CH_2 , 2 CH, 1 OC, 2 C) carbon atoms, accounting for two degrees of unsaturation (Table 2 and Figure S3). The remaining DBEs are indicative of three rings in the molecule. The olefinic proton and two sp^2 carbon signals (δ_H 6.41, H-7; δ_C 148.0, C-7; δ_C 140.1, C-6) were readily recognized as markers for a trisubstituted double bond. The HMBC cross-peak from H-7 to C-13 established an α , β -unsaturated carboxylic acid moiety (Figure 1). The HMBC correlations from H-7 to C-4, C-5, C-6, and C-8, and from allylic proton (δ_H 3.02, H-5) to C-6 permitted the assignment of ring B. Analysis of the COSY spectrum characterized a proton spin system of H₃-10/H-9/H₂-11/H₂-12/H-5. The HMBC cross-peaks from H₃-10 to C-4, C-9, and C-11, and from H-9 to C-5 built ring C. The HMBC correlations from two geminal methyls of H₃-14 and H₃-15 to C-1, C-2, and C-3, from H₂-1 to C-4 and C-8, and from H₂-3 to C-4 and C-5 established the third cyclopentane (ring A).

Table 2. ^1H and ^{13}C -NMR Spectroscopic Data for **1** and **2**^a.

1			2		
no.	δ_{C} , Type	δ_{H} (J in Hz)		δ_{C} , Type	δ_{H} (J in Hz)
1 α	55.3, CH ₂	1.70, d (13.5)	1 α	46.2, CH ₂	1.68, m
1 β		1.87, dd (13.5, 1.3)	1 β		1.68, m
2	38.1, C		2	40.2, C	
3 α	50.1, CH ₂	1.94, d (13.2)	3 α	49.7, CH ₂	2.25, d (14.7)
3 β		1.50, dd (13.2, 1.3)	3 β		1.59, d (14.7)
4	65.4, C		4	65.9, C	
5	60.5, CH	3.02, dd (8.4, 4.4)	5	51.9, CH	3.37, brd (11.2)
6	140.1, C		6	139.8, C	
7	148.0, CH	6.41, s	7	149.8, CH	6.62, brd (2.0)
8	94.4, C		8	55.3, CH	2.94, ddd (7.7, 2.5, 2.0)
9	39.2, CH	2.25, m	9	80.5, C	
10	17.0, CH ₃	0.96, d (7.1)	10	17.1, CH ₃	1.18, s
11 α	35.1, CH ₂	1.72, m	11	217.1, C	
11 β		1.28, dq (12.3, 6.3)			
12 α	31.1, CH ₂	1.44, ddd (18.9, 6.3, 4.4)	12 α	41.2, CH ₂	1.91, dd (18.5, 4.2)
12 β		2.02, m	12 β		3.07, dd (18.5, 11.2)
13	169.2, C		13	167.9, C	
14	27.7, CH ₃	0.94, s	14	31.9, CH ₃	1.09, s
15	32.1, CH ₃	1.06, s	15	30.9, CH ₃	1.04, s

^a In CD₃OD, 600 MHz for ^1H and 150 MHz for ^{13}C -NMR.

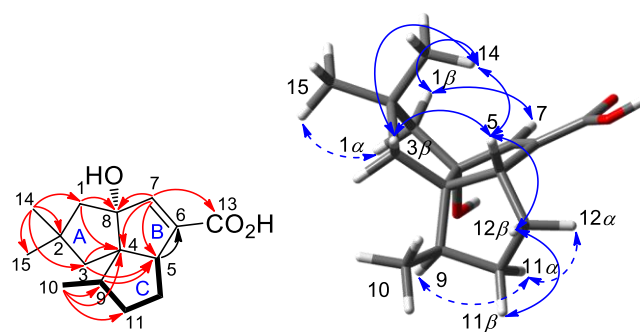


Figure 1. Key COSY (bold), HMBC (red arrows), and NOE (blue arrows) correlations of **1**.

In the NOESY spectrum of **1**, the observed NOE correlations of H-1 β /H₃-14, H-1 β /H-7, H₃-14/H-3 β , H-3 β /H-5, H-5/H₃-14, H-5/H-12 β , and H-12 β /H-11 β indicated a β orientation of these protons (Figure 1). NOE cross-peaks of H-1 α /H₃-15, H-9/H-11 α , and H-11 α /H-12 α revealed that these protons were α oriented. A (4*S**,5*R**,8*R**,9*R**)-**1** relative configuration was then deduced. The absolute configuration was determined by time-dependent density functional theory/electronic circular dichroism (TDDFT/ECD) calculation. The Boltzmann-weighted ECD spectrum showed a good superposition with the experimental curve of **1**, particularly, the positive band at 208 nm and the negative band at 247 nm (Figure 2 and Figure S1). Therefore, **1** was assigned to have a (4*S*,5*R*,8*R*,9*R*) configuration and named as 1-deoxy-8 α -hydroxypentalenic acid.

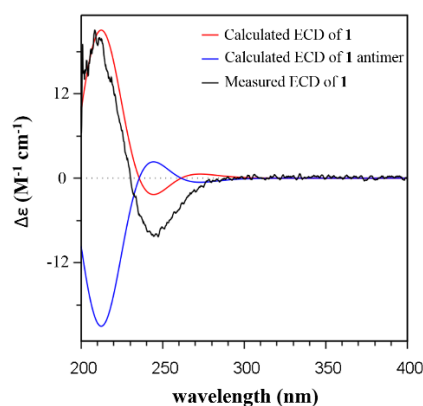


Figure 2. Comparison of the experimental ECD spectra of **1** with the TDDFT-predicted ECD curve of **1** (CAM-B3LYP/6-31g(d) functional/basis set, optimization at the B3LYP/6-31g(d) level).

Compound **2**, a white powder, has a molecular formula of $C_{15}H_{20}O_4$ as determined by HRESIMS at m/z 263.1282 $[M - H]^-$ (calcd for $C_{15}H_{19}O_4$, 263.1278). The 1H and ^{13}C -NMR spectra of **2** showed a close similarity to those of **1**, suggesting a sesquiterpenoid skeleton (Table 2 and Figure S4). A difference was observed with the presence of a ketone group (δ_C 217.1, C-11) in the shielded region of the ^{13}C spectrum and three methyl singlets in the deshielded region of the 1H spectrum. The COSY spectrum indicated the presence of two isolated proton sequences, of $H_2-1/H-8/H-7$ and $H-5/H_2-12$ (Figure 3). The HMBC correlations from H_3-10 to C-4, C-9 (δ_C 80.5), and C-11, and from H_2-12 to C-11 located the ketone group at C-11 and the oxygen-bearing quaternary carbon at C-9. The HMBC correlations from H-7 to C-4, C-5, and C-13 confirmed the presence of α , β -unsaturated carboxylic acid and a B ring. The HMBC cross-peaks from both H_3-14 and H_3-15 to C-1, C-2, C-3, and C-4, and from H_2-1 to C-4 and C-7, and from H_2-3 to C-4 and C-5 confirmed the presence of a complete ring A.

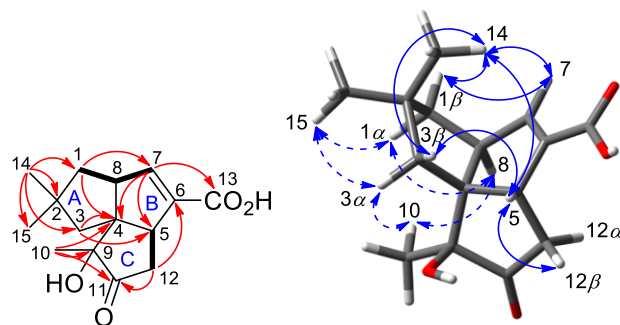


Figure 3. Key COSY (bold), HMBC (red arrows), and NOE (blue arrows) correlations of **2**.

Compound **2** showed a similar NOE pattern to that of **1**. The NOE correlations of $H-1\beta/H_3-14$, $H-1\beta/H-7$, $H-3\beta/H_3-14$, $H-3\beta/H-5$, $H-5/H_3-14$, $H-5/H-12\beta$, and $H-7/H_3-14$ suggested that these protons were in β orientation. The NOE cross-peaks of $H-1\alpha/H_3-15$, $H_3-15/H-3\alpha$, $H-3\alpha/H_3-10$, $H-1\alpha/H-8$, and $H-8/H-10$ indicated α orientation of these protons. The 10-OH group was then deduced to be in β orientation. The relative configuration of **2** was assigned to be $(4R^*,5R^*,8S^*,9R^*)$. The structure of **2** was analyzed with the TDDFT/ECD calculation. The calculated ECD spectrum of **2** exhibited a high similarity with the experimental curve (Figure 4 and Figure S2), which led to the assignment of an absolute configuration of **2** of $(4R,5R,8S,9R)$. Compound **2** was assigned to be 1-deoxy-9 β -hydroxy-11-oxopentalenic acid.

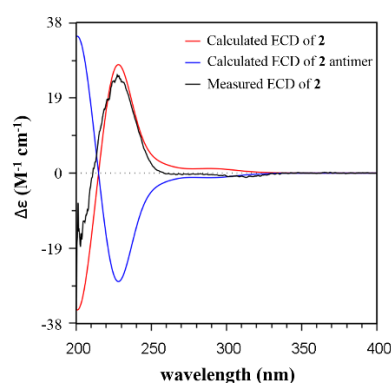


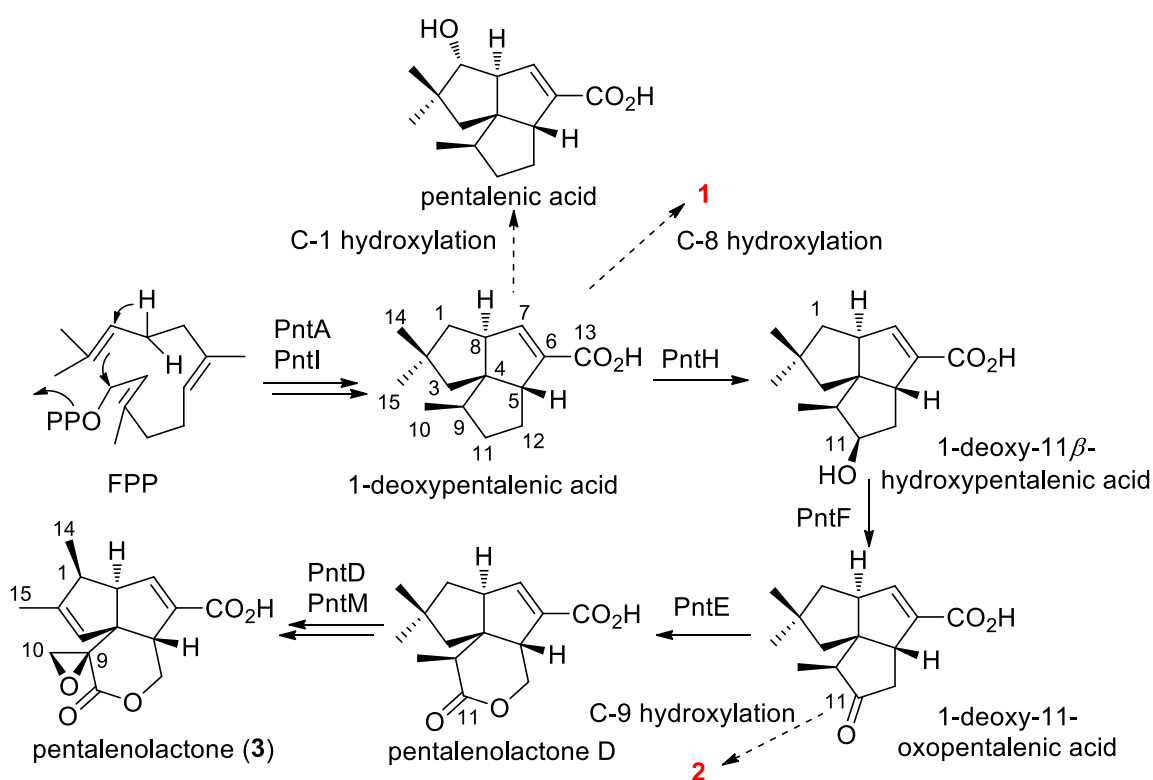
Figure 4. Comparison of the experimental ECD spectra of **2** with the TDDFT-predicted ECD curve of **2** (CAM-B3LYP/6-31g(d) functional/basis set, optimization at the B3LYP/6-31g(d) level).

2.3. Antimicrobial Activity

The two compounds were subsequently evaluated for possible antibacterial activity. Compounds **1** and **2** showed moderate antibacterial activities against Gram-positive bacteria *Staphylococcus aureus* ATCC 25923 with MICs of 16 and 16 $\mu\text{g}/\text{mL}$, and against Gram-negative bacteria *Escherichia coli* ATCC 25922 with MICs of 32 and 16 $\mu\text{g}/\text{mL}$. Kanamycin and ampicillin were used as positive controls with 4 and 2 $\mu\text{g}/\text{mL}$ for *S. aureus* and 16 and 4 $\mu\text{g}/\text{mL}$ for *E. coli*, respectively. The results indicated that the epoxy lactone moiety of pentalenolactone played an important role in the antimicrobial activity.

2.4. Proposed Biosynthetic Pathway

Pentalenolactone (**3**) is a widely occurring sesquiterpenoid antibiotic that has been isolated from a variety of *Streptomyces* species [9–12]. It exhibits antimicrobial action against bacteria, fungi, and protozoa by a reaction of the electrophilic epoxy lactone moiety with the active site cysteine of glyceraldehyde-3-phosphate dehydrogenase [13]. Several pentalenolactone BGCs, e.g., *pen* from *S. exfoliatus*, *pnt* from *S. arenae*, and *ptl* from *S. avermitilis* and biochemical functions of ORFs as well as the biosynthetic pathway have been well characterized by Cane and collaborators (Scheme 1) [14–17]. A high number of biosynthetic intermediates and shunt metabolites in the conversion from farnesyl pyrophosphate (FPP) to pentalenolactone have been isolated from several pentalenolactone producers [14,18,19]. Compounds **1** and **2** can be determined to be in the main pentalenolactone biosynthetic pathway as shunt metabolites. Biosynthetically, PntH, a non-heme iron, α -ketoglutarate-dependent hydroxylase, is responsible for catalyzing 1-deoxypentalenic acid to 1-deoxy-11 β -hydroxypentalenic acid [16]. Compound **1** was assumed to be a shunt metabolite via 8 α hydroxylation of 1-deoxypentalenic acid. Compound **2** might be derived from 1-deoxy-11-oxopentalenic acid via endogenous biotransformation during the fermentation process. A similar phenomenon occurs with pentalenic acid, a common pentalenolactone shunt metabolite isolated from many *Streptomyces* species. In *S. avermitilis*, a cytochrome P450 (CYP105D7) encoded by *sav7469*, which is not present in the *ptl* cluster, was found to be responsible for the conversion of 1-deoxypentalenic acid to pentalenic acid [20]. It is likely that there are some CYPs in S-4 responsible for the formation of **1** and **2**. As the final product, pentalenolactone, was not isolated from S-4, the function of PlIE, a predicted Baeyer-Villiger monooxygenase (BVMO), was bioinformatically examined. The amino acid sequence of PlIE was shown to have 91% identity and 96% similarity to the orthologous PntE [9]. The fingerprint motif FxGxxxHxxxWP/D for type I BVMO and the sequence motif GxGxxG for FAD and NADPH cofactors binding was preserved in PlIE [21]. The reason the final pentalenolactone product was not detected might be partially explained by the instability of the epoxy lactone moiety in pentalenolactone, or by the methods used to process fractions of S-4. The identity of the enzymes responsible for the formation of **1** and **2** requires further investigation.



Scheme 1. The biosynthetic pathway of pentalenolactone and the assumed production of 1 and 2.

3. Materials and Methods

3.1. Fermentation and Isolation

The strain S-4 was inoculated in a 250 mL Erlenmeyer flask containing 100 mL of ISP2 medium and then grown on 10 L of fermentation medium (soybean flour 10 g/L, glucose 10 g/L, soluble starch 15 g/L, yeast extract 5 g/L, NaCl 5 g/L, CaCO₃ 3 g/L, pH 7.0) at 28 °C for 7 days. Using the same isolation procedure [6], the EtOAc extract of S-4 was subjected to CC on ODS to afford 13 fractions (Frs. 1–13). Fr.8 was fractionated by Sephadex LH-20 (CH₂Cl₂/MeOH, 2:1) followed by RP-HPLC (60% MeOH, 1.5 mL/min) to give compounds 1 (6.0 mg, *t_R* 40.3 min) and 2 (17.2 mg, *t_R* 36.1 min).

Compound 1: white amorphous powder; *R_f* 0.39 (CH₂Cl₂/MeOH 15:1); [α]^{28.7}_D -30 (*c* 0.1, MeOH); UV (MeCN) λ_{max} (log ε) 213 (3.45) nm; ECD (*c* 3.1 × 10⁻⁵, MeCN) λ_{max} (Δε) 208 (15.9), 247 (-6.3) nm; IR (film) ν_{max} 3377, 2951, 2926, 1689, 1366, 1251, 1053, 755 cm⁻¹. ¹H and ¹³C-NMR data see Table 2; HRESIMS *m/z*: 249.1489 [M - H]⁻ (calcd for C₁₅H₂₁O₃, 249.1485), 273.1512 [M + Na]⁺, 233.1587 [M + H - H₂O]⁺.

Compound 2: white amorphous powder; *R_f* 0.40 (CH₂Cl₂/MeOH 15:1); [α]^{29.3}_D +8.4 (*c* 0.05, MeOH); UV (MeCN) λ_{max} (log ε) 220 (3.69) nm; ECD (*c* 3.1 × 10⁻⁵, MeCN) λ_{max} (Δε) 203 (-18.6), 227 (24.9) nm; IR (film) ν_{max} 3385, 2952, 2932, 1684, 1367, 1216, 1080, 750 cm⁻¹. ¹H and ¹³C-NMR data see Table 2; HRESIMS *m/z*: 263.1282 [M - H]⁻ (calcd for C₁₅H₁₉O₄, 263.1278), 287.1325 [M + Na]⁺, 247.1386 [M + H - H₂O]⁺.

3.2. General Experimental Procedures

Optical rotations were measured on a Rudolph Autopol I polarimeter at the sodium D line (589 nm). UV absorption spectra were recorded with a Varian Cary 100 UV/vis spectrophotometer (Rudolph Research Analytical, Splendora, TX, USA); wavelengths were reported in nm. ECD spectra were recorded with a Jasco-810 spectropolarimeter (JASCO Corporation, Japan). Infrared spectra were recorded in thin polymer films on a Thermo Nicolet Nexus 470 FT-IR spectrophotometer (Thermo Nicolet Corporation, USA); peaks were reported in cm⁻¹. NMR data were acquired at 300K on a Bruker Avance DRX-600

NMR spectrometer (Bruke Magnetic Resonance, Germany). Chemical shifts were reported relative to the residual CD₃OD signals (δ_{H} 3.31; δ_{C} 49.0) as an internal standard for ¹H and ¹³C-NMR spectra. The HRESIMS data were acquired on an Agilent 6224 TOF LC-MS (Agilent Technologies Inc., USA), resolution 5000, equipped with an electrospray ionization source. Semi-preparative HPLC was performed on an Agilent 1100 system with UV and refractive index detectors using a YMC Pack ODS-A column (250 × 10 mm, 5 μm) (Agilent Technologies Inc., USA). Commercial silica gel (200–300 mesh) and Sephadex LH-20 (GE Healthcare, Bio-Sciences AB, Sweden). were used for column chromatography (CC). Pre-coated silica gel plates (HSGF-254) were used for thin-layer chromatography (TLC) and spots were detected under UV or by heating after spraying with an anisaldehyde sulfuric acid reagent.

3.3. ECD Calculations

Conformational analysis within an energy window of 3.0 kcal/mol was performed by using the OPLS3 molecular mechanics force field via the MacroModel panel of Maestro 10.2 [22]. The conformers were then further optimized with the software package Gaussian 09 [23] at the B3LYP/6-31G(d) level, and the harmonic vibrational frequencies were calculated to confirm their stability. Then, the 60 lowest electronic transitions for the obtained conformers in a vacuum were calculated using TDDFT methods at the CAM-B3LYP/6-31G(d) level. ECD spectra of the conformers were simulated using a Gaussian function. The overall theoretical ECD spectra were obtained according to the Boltzmann weighting of each conformer.

3.4. Antimicrobial Activity Assays

Antimicrobial activity was evaluated against Gram-positive bacteria *S. aureus* ATCC 25923 and Gram-negative bacteria *E. coli* ATCC 25922. MIC values for test compounds were assessed using a 96-well plate format with LB broth (tryptone 10 g/L, yeast extract 5.0 g/L, NaCl 10 g/L, pH 7.2), using a 2-fold dilution method. The test compounds were first dissolved in DMSO at a concentration of 3.2 mg/mL, and this was diluted to 128 μg/mL with LB broth. Then, sequential 2-fold serial dilutions of the mixture were carried out in 100 μL of LB broth, and 100 μL of cell cultures were added to each of the wells. After incubation at 37 °C for 16–18 h, the lowest concentrations that completely inhibited the growth of bacteria were detected by microplate reader for each of the test compounds. All assays were carried out in triplicate.

4. Conclusions

In summary, the analysis of genome data of S-4 showed the presence of terpenoid BGCs. Furthermore, two new terpenoids, 1-deoxy-8 α -hydroxypentalenic acid (**1**) and 1-deoxy-9 β -hydroxy-11-oxopentalenic acid (**2**), were isolated and characterized from the target strain. The discovery of **1** and **2** confirmed that the pentalenolactone pathway was functional in this organism. Compounds **1** and **2** might be shunt metabolites of the main pentalenolactone biosynthesis pathway. In the bioactivity screening, **1** and **2** exhibited moderate antibacterial activities against both Gram-positive and Gram-negative bacteria. The current results validated the biosynthetic potential of Actinobacteria to produce terpenoids. The application of genome mining in this study facilitated the exploration of Actinobacteria as one of the most promising sources of natural drug discovery.

Supplementary Materials: The following are available online: BGC clusters of S-4, The optimized conformers, HRESIMS and NMR spectra of **1** and **2**. Figure S1: The optimized conformers of **1** and Boltzmann populations (>1%), Figure S2: The optimized conformers of **2** and Boltzmann populations (>1%), Figure S3: MS and NMR spectra of **1**, Figure S4: MS and NMR spectra of **2**, Table S1: Biosynthetic gene clusters in *Streptomyces* sp. NRRL S-4.

Author Contributions: H.L. (Huanhuan Li) contributed in isolation and characterization of compounds. H.L. (Hongji Li) and S.C. drafted the initial version of the manuscript. W.W. contributed in

literature searching. P.S. supervised and revised the manuscript. All authors have read and agreed to the published version of the manuscript.

Funding: This work was financially supported by National Natural Science Foundation of China (41876184) and the National Key R&D Program of China (2019YFC0312601 and 2019YFC0312502).

Institutional Review Board Statement: Not applicable.

Informed Consent Statement: Not applicable.

Data Availability Statement: The data presented in this study are available in article and Supplementary Material.

Acknowledgments: Not applicable.

Conflicts of Interest: The authors declare no conflict of interest.

Sample Availability: Samples of the compounds **1** and **2** are available from the authors.

References

1. Musiol-Kroll, E.M.; Tocchetti, A.; Sosio, M.; Stegmann, E. Challenges and advances in genetic manipulation of filamentous actinomycetes—the remarkable producers of specialized metabolites. *Nat. Prod. Rep.* **2019**, *36*, 1351–1369. [[CrossRef](#)] [[PubMed](#)]
2. Yamada, Y.; Kuzuyama, T.; Komatsu, M.; Shin-Ya, K.; Omura, S.; Cane, D.E.; Ikeda, H. Terpene synthases are widely distributed in bacteria. *Proc. Natl. Acad. Sci. USA* **2015**, *112*, 857–862. [[CrossRef](#)]
3. Medema, M.H.; de Rond, T.; Moore, B.S. Mining genomes to illuminate the specialized chemistry of life. *Nat. Rev. Genet.* **2021**, *22*, 553–571. [[CrossRef](#)]
4. Geng, W.-L.; Wang, X.-Y.; Kurtán, T.; Mándi, A.; Tang, H.; Schulz, B.; Sun, P.; Zhang, W. Herbarone, a rearranged heptaketide derivative from the sea hare associated fungus *Torula herbarum*. *J. Nat. Prod.* **2012**, *75*, 1828–1832. [[CrossRef](#)] [[PubMed](#)]
5. Sun, P.; Xu, D.-X.; Mándi, A.; Kurtán, T.; Li, T.-J.; Schulz, B.; Zhang, W. Structure, absolute configuration, and conformational study of 12-membered macrolides from the fungus *Dendrodochium* sp. associated with the sea cucumber *Holothuria nobilis* Selenka. *J. Org. Chem.* **2013**, *78*, 7030–7047. [[CrossRef](#)]
6. Li, H.; Zhang, M.; Li, H.; Yu, H.; Chen, S.; Wu, W.; Sun, P. Discovery of venturicin congeners and identification of the biosynthetic gene cluster from *Streptomyces* sp. NRRL S-4. *J. Nat. Prod.* **2021**, *84*, 110–119. [[CrossRef](#)] [[PubMed](#)]
7. Frattaruolo, L.; Lacroet, R.; Cappello, A.R.; Truman, A.W. A genomics-based approach identifies a thioviridamide-like compound with selective anticancer activity. *ACS Chem. Biol.* **2017**, *12*, 2815–2822. [[CrossRef](#)]
8. Blin, K.; Shaw, S.; Steinke, K.; Villebro, R.; Ziemert, N.; Lee, S.Y.; Medema, M.H.; Weber, T. antiSMASH 5.0: Updates to the secondary metabolite genome mining pipeline. *Nucleic Acids Res.* **2019**, *47*, W81–W87. [[CrossRef](#)]
9. Seo, M.J.; Zhu, D.; Endo, S.; Ikeda, H.; Cane, D.E. Genome mining in *Streptomyces*. Elucidation of the role of Baeyer-Villiger monooxygenases and non-heme iron-dependent dehydrogenase/oxygenases in the final steps of the biosynthesis of pentalenolactone and neopentalenolactone. *Biochemistry* **2011**, *50*, 1739–1754. [[CrossRef](#)]
10. Koe, B.K.; Sobin, B.A.; Celmer, W.D. PA 132, a new antibiotic. I. Isolation and chemical properties. *Antibiot. Annu.* **1957**, 672–675.
11. Takeuchi, S.; Ogawa, Y.; Yonehara, H. The structure of pentalenolactone (PA-132). *Tetrahedron Lett.* **1969**, *32*, 2737–2740.
12. Martin, D.; Slomp, G.; Mizsak, S.; Duchamp, D.; Chidester, C. The structure and absolute configuration of pentalenolactone (PA 132). *Tetrahedron Lett.* **1970**, *56*, 4901–4904. [[CrossRef](#)]
13. Duszynko, M.; Balla, H.; Mecke, D. Specific inactivation of glucose metabolism from eucaryotic cells by pentalenolactone. *Biochim. Biophys. Acta* **1982**, *714*, 344–350. [[CrossRef](#)]
14. Quaderer, R.; Omura, S.; Ikeda, H.; Cane, D.E. Pentalenolactone biosynthesis. Molecular cloning and assignment of biochemical function to PtlI, a cytochrome P450 of *Streptomyces avermitilis*. *J. Am. Chem. Soc.* **2006**, *128*, 13036–13037. [[CrossRef](#)] [[PubMed](#)]
15. Tetzlaff, C.N.; You, Z.; Cane, D.E.; Takamatsu, S.; Omura, S.; Ikeda, H. A gene cluster for biosynthesis of the sesquiterpenoid antibiotic pentalenolactone in *Streptomyces avermitilis*. *Biochemistry* **2006**, *45*, 6179–6186. [[CrossRef](#)] [[PubMed](#)]
16. You, Z.; Omura, S.; Ikeda, H.; Cane, D.E. Pentalenolactone biosynthesis. molecular cloning and assignment of biochemical function to PtlH, a non-heme iron dioxygenase of *Streptomyces avermitilis*. *J. Am. Chem. Soc.* **2006**, *128*, 6566–6567. [[CrossRef](#)] [[PubMed](#)]
17. Duan, L.; Jögl, G.; Cane, D.E. The cytochrome P450-catalyzed oxidative rearrangement in the final step of pentalenolactone biosynthesis: Substrate structure determines mechanism. *J. Am. Chem. Soc.* **2016**, *138*, 12678–12689. [[CrossRef](#)]
18. Seto, H.; Sasaki, T.; Yonehara, H.; Takahashi, S.; Takeuchi, M.; Kuwano, H.; Arai, M. Studies on the biosynthesis of pentalenolactone. VII. Isolation of pentalenolactones P and O. *J. Antibiot.* **1984**, *37*, 1076–1078. [[CrossRef](#)]
19. Cane, D.E.; Sohng, J.K.; Williard, P.G. Isolation and structure determination of pentalenolactones A, B, D, and F. *J. Org. Chem.* **1992**, *57*, 844–851. [[CrossRef](#)]
20. Takamatsu, S.; Xu, L.H.; Fushinobu, S.; Shoun, H.; Komatsu, M.; Cane, D.E.; Ikeda, H. Pentalenic acid is a shunt metabolite in the biosynthesis of the pentalenolactone family of metabolites: Hydroxylation of 1-deoxypentalenic acid mediated by CYP105D7 (SAV_7469) of *Streptomyces avermitilis*. *J. Antibiot.* **2011**, *64*, 65–71. [[CrossRef](#)]

-
21. Rebehmed, J.; Alphan, V.; de Berardinis, V.; de Brevern, A.G. Evolution study of the Baeyer-Villiger monooxygenases enzyme family: Functional importance of the highly conserved residues. *Biochimie* **2013**, *95*, 1394–1402. [[CrossRef](#)] [[PubMed](#)]
 22. Frisch, M.J.; Trucks, G.W.; Schlegel, H.B.; Scuseria, G.E.; Robb, M.A.; Cheeseman, J.R.; Scalmani, G.; Barone, V.; Mennucci, B.; Petersson, G.A.; et al. *Gaussian 09, Revision B.01*; Gaussian, Inc.: Wallingford, CT, USA, 2010.
 23. *MacroModel 10.2*; Schrödinger, LLC: New York, NY, USA, 2009.